Biatrial remodelling in atrial fibrillation: A three-dimensional and strain echocardiography insight

Laurie Soulat-Dufour, Sylvie Lang, Stephane Ederhy, Yann Ancedy, Anne-Sophie Beraud, Saroumadi Adavane-Scheuble, Marion Chauvet-Droit, Nadjib Hammoudi, Aliocha Scheuble, Pascal Nhan, et al.

Biatrial remodelling in atrial fibrillation: A three-dimensional and strain echocardiography insight

Remodelage biatrial dans la fibrillation atriale : intérêt de l'échographie tridimensionnelle et du strain

Abbreviated title: Biatrial remodelling in atrial fibrillation

Laurie Soulat-Dufour[a,b], Sylvie Lang[a], Stephane Ederhy[a], Yann Ancedy[a], Anne-Sophie Beraud[c], Saroumadi Adavane-Scheuble[a], Marion Chauvet-Droit[a], Nadjib Hammoudi[b,d], Aliocha Scheuble[e], Pascal Nhan[a], Magali Charbonnier[a], Franck Boccara[a,f], Ariel Cohen[a,b,*]

[a] *Service de Cardiologie, Hôpital Saint-Antoine, AP-HP, Hôpitaux de l'Est Parisien, Sorbonne Universités, 75012 Paris, France*

[b] *INSERM, UMRS-ICAN 1166 "Unité de recherche sur les maladies cardiovasculaires, du métabolisme et de la nutrition", 75013 Paris, France*

[c] *Clinique Pasteur, 31076 Toulouse, France*

[d] *Service de Cardiologie, Hôpital Pitié-Salpêtrière, Sorbonne Universités, 75013 Paris, France*

[e] *Centre Cardiologique du Nord, 93200 Saint-Denis, France*

[f] *INSERM, UMR S 938, Centre de Recherche Saint-Antoine, 75012, Paris, France*

* Corresponding author at: Service de Cardiologie, Hôpital Saint-Antoine, AP-HP, 184 rue du Faubourg Saint-Antoine, 75012 Paris CEDEX 12, France.

E-mail address: ariel.cohen@aphp.fr (A. Cohen).

Summary

Background. – Atrial remodelling has been poorly investigated in atrial fibrillation (AF), and few studies have focused on biatrial remodelling.

Aim. – To evaluate right atrial (RA) and left atrial (LA) remodelling in AF using global atrial reservoir strain and three-dimensional (3D) atrial volumes, according to rhythm outcome at mid-term follow-up.

Methods. – Two-dimensional and 3D transthoracic echocardiography (TTE) were performed within 24 hours after admission (M0) and at 6-month follow-up (M6) in patients admitted for AF. RA and LA variables were assessed: body surface area-indexed maximum 3D volume (Max 3D RA Vol_i, Max 3D LA Vol_i) and minimum 3D volume (Min 3D RA Vol_i, Min 3D LA Vol_i); atrial emptying fraction (3D RAEF, 3D LAEF); atrial expansion index (3D RAEI, 3D LAEI); and global RA and LA reservoir strain.

Results. – Forty-eight consecutive patients were included prospectively. Three groups were identified depending on rhythm at M0 and M6: AF at M0 and sinus rhythm (SR) at M6 (AF-SR) in 25 (52.1%) patients; AF at M0 and AF at M6 (AF-AF) in 13 (27.1%) patients; and SR at M0 (spontaneous cardioversion before first TTE) and SR at M6 (SR-SR) in 10 (20.8%) patients. Between M0 and M6 in the AF-SR group, we found: significant decreases in Max 3D RA Vol_i ($P = 0.020$), Min 3D RA Vol_i ($P = 0.0008$), Max 3D LA Vol_i ($P = 0.001$) and Min 3D LA Vol_i ($P = 0.0021$); significant increases in 3D RAEF ($P = 0.037$) and 3D RAEI ($P = 0.034$); no significant differences in 3D LAEF and 3D LAEI; and significant increases in global RA and LA reservoir strain (both $P < 0.0001$). There was no significant difference with regard to these variables in the AF-AF and SR-SR groups.

Conclusion. – 3D volume and strain analyses were useful in the evaluation of RA and LA reverse remodelling in successfully cardioverted patients with AF.

Résumé

Contexte. – Le remodelage atrial a été peu étudié dans la fibrillation atriale (FA) et peu d'études ont ciblé plus spécifiquement le remodelage biatrial.

But. – Evaluer le remodelage de l'oreillette droite (OD) et de l'oreillette gauche (OG) dans la fibrillation atriale (FA) en utilisant le strain atrial global pendant la phase réservoir et les volumes atriaux en échocardiographie 3D selon le rythme du patient à moyen terme

Méthodes. – Une échocardiographie complète 2D et 3D était réalisé dans les 24h (M0) et à 6 mois (M6) du suivi chez des patients admis pour FA. Les paramètres OD et OG étaient évalués : volume

3D maximum (Max 3D OD Vol_i, Max 3D OG Vol_i) et volume 3D minimum (Min 3D OD Vol_i, Min 3D OG Vol_i) indexés à la surface corporelle, fraction de vidange des oreillettes (3D FVOD, 3D FVOG), index d'expansion des oreillettes (3D IEOD, 3D IEOG) et strain global réservoir de l'OD et de l'OG.

Résultats. – Quarante-huit patients consécutifs ont été prospectivement inclus. Trois groupes ont été identifiés selon le rythme à M0 et M6 : FA à M0 et rythme sinusal (RS) à M6 (FA-RS) chez 25 (52,1 %) patients ; FA à M0 et FA à M6 (FA-FA) chez 13 (27,1 %) patients ; et RS à M0 (cardioversion spontanée avant la première ETT) et RS à M6 (RS-RS) chez 10 (20,8 %) patients. Entre M0 et M6 dans le groupe FA-RS, nous avons trouvé : une diminution significative du Max 3D OD Vol_i (P = 0,020), Min 3D OD Vol_i (P = 0,0008), Max 3D OG Vol_i (P = 0,001) et du Min 3D OG Vol_i (P = 0,0021) ; une augmentation significative de la 3D FVOD (P = 0,037) et du 3D IEOD (P = 0,034) ; pas de différence significative de la 3D FVOG et du 3D IEOG ; et il existe une augmentation significative du strain global réservoir de l'OD et de l'OG (P < 0,0001 pour les 2 paramètres). Il n'y a pas de différence significative pour l'ensemble de ces paramètres dans le groupe FA-FA et RS-RS.

Conclusion. – L'analyse des paramètres en 3D et du strain peuvent être utiles pour évaluer le remodelage inverse de l'OD et de l'OG chez les patients présentant un succès de cardioversion de FA.

KEYWORDS

Atrial function;

Atrial remodelling;

Atrial strain;

3D echocardiography;

Atrial fibrillation

MOTS CLÉS

Fonction atriale ;

Remodelage atrial ;

Strain atrial ;

Échocardiographie 3D ;

Fibrillation atriale

Abbreviations: 2D, two-dimensional; 3D, three-dimensional; AF, atrial fibrillation; LA, left atrial; LAEF, left atrial emptying fraction; LAEI, left atrial expansion index; Max 3D LA Vol_i, body surface area-indexed minimal three-dimensional left atrial volume; Max 3D RA Vol_i, body surface area-indexed minimal three-dimensional right atrial volume; Min 3D LA Vol_i, body surface area-indexed minimal three-dimensional left atrial volume; Min 3D RA Vol_i, body surface area-indexed minimal three-dimensional right atrial volume; MRI, magnetic resonance imaging; RA, right atrial; RAEF, right atrial emptying fraction; RAEI, right atrial expansion index; SR, sinus rhythm; TTE, transthoracic echocardiography.

Background

The relationship between left atrial (LA) size and non-valvular atrial fibrillation (AF) has been established. Data from the Framingham study identified LA size as an independent echocardiographic predictor of AF [1]. Currently, in addition to LA size, LA function can be evaluated using three-dimensional (3D) volumetric or two-dimensional (2D) strain atrial variables [2]. Increased atrial size and impaired atrial function are hallmarks of atrial remodelling, an important underlying substrate in AF [3]. The atrial remodelling process is complex and poorly understood, and includes atrial fibrosis, hypocontractility, fatty infiltration, inflammation, vascular remodelling, ischaemia, ion channel dysfunction and Ca^{2+} instability [3, 4]. The term "atrial cardiomyopathy" has been suggested to refer to "any complex of structural, architectural, contractile, or electrophysiological changes affecting the atria with the potential to produce clinically relevant manifestations" [5].

Previous studies have described the potential role of transthoracic echocardiography (TTE) in the evaluation of LA remodelling in AF in several clinical settings: to determine the effect on LA size, volume and function, before and after catheter ablation [6]; to identify patients with a high risk of AF recurrence [7]; and, more recently, to predict AF in cryptogenic cerebrovascular accidents [8, 9]. Finally, right atrial (RA) remodelling has been poorly investigated in AF, and few studies have focused on biatrial remodelling in AF [10, 11].

In this study, we sought to evaluate LA and RA remodelling in AF using TTE-derived global atrial reservoir strain and 3D atrial volumes, according to rhythm outcome at mid-term follow-up.

Methods

Study population

The FASTRHAC study (Fibrillation Atriale et STRatification du risque thrombo-embolique et Hémorragique des patients sous AntiCoagulant) is a French national multicentre study of patients hospitalized for non-valvular AF since July 2015 (inclusion still in progress). The study is being conducted in compliance with local regulations, French laws regarding patient care (act of 04 March 2002 on patients' rights) and the principle of the Declaration of Helsinki. Informed written consent was obtained from all patients.

Inclusion criteria were: documented paroxysmal, persistent or permanent AF on electrocardiography; age > 18 years; and provision of patient consent. Exclusion criteria were: valvular

AF (mitral stenosis, defined as an area < 2 cm^2; mitral, aortic or tricuspid regurgitation greater than moderate to severe; moderate or severe aortic stenosis; mechanical or biological prosthesis); contraindication to anticoagulant treatment; no affiliation to a social security regimen; severe psychiatric history; or unlikelihood to attend follow-up.

A comprehensive physical examination and electrocardiogram were carried out and clinical data were collected at admission and every 6 months for 2 years. Biological samples were collected at admission and 1 year after admission. Comprehensive TTE and transoesophageal echocardiography were performed within 24 hours after admission (M0). Comprehensive TTE was repeated every 6 months for 2 years, and comprehensive transoesophageal echocardiography at 1-year and 2-year follow-up.

In this study, the first forty-eight consecutive patients enrolled in the FASTRHAC study were analysed at M0 and at 6-month follow-up (M6) to evaluate TTE results of atrial strain and 3D atrial volumes in AF, and biatrial remodelling at 6-month follow-up.

TTE

2D analysis

Comprehensive TTE examinations were performed at M0 and M6. TTE was always performed by experienced cardiologists using an X5-1 transducer on the iE33 system or an X5-1 transducer on the EPIQ system (Philips Medical Systems, Andover, MA, USA). The data were transferred and analysed offline using the IntelliSpace CardioVascular (ISCV) workstation (Philips Medical Systems). All images and measurements were performed using standard views, according to American Society of Echocardiography and European Association of Cardiovascular Imaging guidelines [12]. Three to five consecutive cardiac cycles were recorded and averaged, and all volumetric measures were indexed to body surface area.

3D analysis

3D full-volume and high-volume rate acquisitions were performed in the four-chamber view during end-expiratory apnoea, to evaluate 3D atrial volumes. The frame rate was set to between 20 and 35 frames/s. The 3D data sets were stored digitally, and quantitative analyses were performed offline (QLAB Advanced Cardiac 3D Quantification software, version 10.7; Philips Medical Systems). The LA

endocardium was defined on two orthogonal planes to obtain non-foreshortened views of the LA. The endocardial surfaces of the atria were drawn by a semiautomated contour tracing algorithm developed for the left ventricle.

3D TTE was used to determine: (1) body surface area-indexed minimal RA volume (Min 3D RA Vol_i) (defined as the volume immediately after tricuspid closure) and body surface area-indexed maximal RA volume (Max 3D RA Vol_i) (defined as the volume immediately before tricuspid valve opening); and (2) body surface area-indexed minimal 3D LA volume (Min 3D LA Vol_i) (defined as the volume immediately after mitral closure) and body surface area-indexed maximal 3D LA volume (Max 3D LA Vol_i) (defined as the volume immediately before mitral valve opening). 3D TTE was also used to evaluate atrial function using the following formulae: 3D RA emptying fraction (3D RAEF) = ([Max 3D RA Vol_i – Min 3D RA Vol_i] / Max 3D RA Vol_i) × 100; 3D LA emptying fraction (3D LAEF) = ([Max 3D LA Vol_i – Min 3D LA Vol_i] / Max 3D LA Vol_i) × 100; 3D RA expansion index (3D RAEI) = (Max 3D RA Vol_i – Min 3D RA Vol_i] / Min 3D RA Vol_i) × 100; and 3D LA expansion index (3D LAEI) = (Max 3D LA Vol_i – Min 3D LA Vol_i] / Min 3D LA Vol_i) × 100.

Strain analysis

RA and LA reservoir strain were analysed using semiautomated software developed for the left ventricle (QLAB Automated Cardiac Motion Quantification software, version 10.7; Philips Medical Systems). Three to five consecutive cardiac cycles were recorded and averaged. The frame rate was set between 60 and 80 frames/s. The initiation of strain calculation was chosen as the onset of the QRS complex (R-R gating), as proposed in most studies [13].

The endocardial surfaces of the atria were drawn by a semiautomated contour tracing algorithm: first, the operator manually defined the septal, lateral and apex of the atrium, and then the software automatically generated a region of interest in a four-chamber view for the RA, and in four-chamber and two-chamber views for the LA; these were manually adjusted, as needed, to allow for adequate speckle tracking. Three patterns of atrial strain were recorded in patients in sinus rhythm (SR): the first peak between the R wave and the T wave was the reservoir strain; the second peak, starting on the P wave, was the contractile strain (atrial systole); and finally, the difference between reservoir strain and contractile strain values reflected the conduit strain [14] (Fig. 1). In AF, only the reservoir strain was determined because of the loss of atrial systole and thus the loss of contractile strain [15] (Fig. 1).

The software divided the region of interest into seven segments in the four-chamber and two-chamber views, and a regional longitudinal strain was generated for each segment. The global longitudinal strain of each apical view was calculated as a weighted combination of the regional strains (related to the length of each segment). The RA global longitudinal strain was the global longitudinal strain derived from the RA four-chamber view. The LA mean global longitudinal strain was calculated as the average of the global longitudinal strain from the LA four-chamber and LA two-chamber views. The atrial global longitudinal strain was considered as not evaluable if more than one segment in the apical view was inadequate or if not assessed concomitantly in four-chamber and two-chamber views for LA global longitudinal strain.

All TTEs were reviewed by one observer who was experienced in strain imaging and 3D echocardiography (L. S.-D.), and evaluation of atrial strain and atrial 3D volumes was performed in all patients at M0 and M6.

Reproducibility

Intraobserver and interobserver variability for atrial 3D volume and atrial strain were assessed in 10 randomly selected subjects. Intraobserver variability was tested by one observer (L. S.-D.) who reanalysed the same images 6 months apart, blinded to the first measurements. For interobserver variability, two observers (L. S.-D. and Y. A.) analysed the same images, and were blinded to the other observer's measurements and to the outcome at M6.

Statistical analysis

The baseline characteristics of the patients, stratified by cardiac rhythm at M0 and M6 follow-up, are presented as means ± standard deviations or medians (25^{th} and 75^{th} percentiles) for continuous data, and as absolute numbers and percentages for categorical data. The Kruskal-Wallis rank-test was used to compare continuous variables, and Fisher's exact test was used to compare categorical variables. Comparison between inclusion and follow-up echocardiographic data measurements was done using the paired *t*-test after assessment of the normal distribution of the data using the Shapiro-Wilk test. The results are presented as means ± standard errors. Intraobserver and interobserver variability of the echocardiographic measurements were evaluated using the concordance correlation coefficient and Bland-Altman plots. A two-sided *P* value ≤ 0.05 was considered statistically significant. All

analyses were performed using STATA V12 statistical software (StataCorp, College Station, TX, USA).

Results

Study population

Forty-eight consecutive patients hospitalized for non-valvular AF were included prospectively. The population was divided depending on the rhythm at M0 and M6: AF at M0 and SR at M6 (AF-SR) in 25 (52.1%) patients; AF at M0 and AF at M6 (AF-AF) in 13 (27.1%) patients; SR at M0 (spontaneous cardioversion before the first TTE) and SR at M6 (SR-SR) in 10 (20.8%) patients. No patient was in SR at M0 and AF at M6 (Fig. 2).

The mean age of the population was 62.7 ± 11.7 years, 36 (75.0%) patients were men, and the CHA_2DS_2-VASc (congestive heart failure, hypertension, age ≥ 75 years [doubled], diabetes mellitus, stroke/transient ischaemic attack/thromboembolism [doubled], vascular disease, age 65–74 years, sex category [female]) risk score was ≥ 2 in 32 (66.7%) patients. There were significant differences across the groups in terms of history of AF and heart failure. There was no significant difference between the three groups according to the other variables (including heart rate, cardiovascular risk factors, CHA_2DS_2-VASc score, B-type natriuretic peptide, troponin, C-reactive protein, D-dimer, M0 TTE variables and treatment at discharge) (Table A.1).

Structural reverse remodelling: 3D volume analysis

At M0 and M6, 3D RA volume was assessed in 33 (68.8%) patients, and 3D LA volume was assessed in 35 (72.9%) patients (Table 1). Between M0 and M6, in the AF-SR group, we found a significant decrease in Max 3D RA Vol_i ($P = 0.020$) and Min 3D RA Vol_i ($P = 0.0008$), and in Max 3D LA Vol_i ($P = 0.001$) and Min 3D LA Vol_i ($P = 0.0021$). There were no significant differences with regard to these variables in the SR-SR and AF-AF groups (Table 1).

Functional reverse remodelling

3D volume analysis

Between M0 and M6, in the AF-SR group, we found a significant increase in 3D RAEF ($P = 0.037$) and 3D RAEI ($P = 0.034$). There were no significant differences with regard to these variables in the AF-AF and SR-SR groups (Table 2). There were also no significant differences in the AF-SR, AF-AF and SR-SR groups for 3D LAEF and 3D LAEI (Table 2).

Strain analysis

At M0 and M6, global RA strain was assessed in all patients, and mean global LA strain was assessed in 40 (83.3%) patients. Between M0 and M6, in the AF-SR group, we found significant increases in global RA and LA reservoir strains (both $P < 0.0001$), but no significant differences in the AF-AF and SR-SR groups (Fig. 3).

Reproducibility

The reproducibility of atrial 3D volume and atrial strain was good, with a concordance correlation coefficient ± standard error between 0.88 ± 0.07 and 0.98 ± 0.01 for intraobserver reproducibility and between 0.68 ± 0.15 and 0.96 ± 0.03 for interobserver reproducibility (Table A.2).

Discussion

In this prospective observational study, we demonstrated significant structural and functional reverse remodelling of the left and right atria, evaluated by 2D echocardiography (strain analysis) and 3D echocardiography (3D atrial volume), in patients with AF who were successfully cardioverted.

LA remodelling

LA structural and functional remodelling have been described previously in patients with AF, using TTE. Maintenance of SR after radiofrequency catheter ablation results in structural remodelling, with a reduction in the 2D LA area/diameter [16-18], 2D LA volume [11, 19-22] and 3D LA volume [23-26], assessed by 2D and 3D TTE. We found similar results in our study among patients with AF who were successfully cardioverted, with reverse LA structural remodelling at 6 months, characterized by a significant decrease in LA 3D volumes.

Other studies have demonstrated the potential of LA strain to analyse LA functional remodelling and identify patients at high risk of AF recurrence among individuals who were candidates for catheter

ablation. Ma et al. [7], in a meta-analysis of eight studies, demonstrated that patients with recurrence of AF were characterized by lower LA strain compared with patients without AF recurrence. In our study, we found a significant improvement in LA strain between M0 and M6 exclusively in the AF-SR group. Thus, we confirmed the potential positive impact of cardioversion on LA functional reverse remodelling. Of note in this group, no significant differences were observed with regard to 3D LAEF or 3D LAEI, probably because of lack of power as a result of the small size of our population sample.

RA remodelling

One key finding in our study was the observation of RA reverse remodelling in addition to LA reverse remodelling. Indeed, RA structural and functional remodelling have been poorly investigated in AF. AF causes biatrial enlargement [27], and restoration of SR after ablation or cardioversion leads to biatrial reverse remodelling, with few reported data on RA structural and functional remodelling. An electrophysiology study [28] with detailed biatrial electroanatomic mapping has demonstrated that AF is associated with remodelling processes affecting both atria. The observed RA remodelling could be an accurate correlate of LA remodelling [28].

RA structural remodelling in AF has been evaluated using TTE [10] and magnetic resonance imaging (MRI) [11, 29]. These studies demonstrated a significant decrease in 3D RA volume after restoration of SR. In a study by Therkelsen et al. [29], only the RA volume normalized 180 days after cardioversion in comparison with healthy volunteers. This may underline the greater and faster ability of the RA to reverse structural remodelling. In our study, we also observed RA structural reverse remodelling restricted to the AF-SR group at M6, with significant decreases in both Max 3D RA Vol_i and Min 3D RA Vol_i, to the same extent as observed with LA reverse remodelling.

To our knowledge, only MRI studies [11, 29] have evaluated RA functional reverse remodelling in AF, and demonstrated a significant increase in 3D RAEF after restoration of SR. In our study, we also found significant increases in 3D RAEF, 3D RAEI, and global RA reservoir strain between M0 and M6 in the AF-SR group only.

Strain and 3D analysis in AF

Most studies of atrial strain or 3D analysis in AF have only included patients with paroxysmal AF, and echocardiographic variables were analysed during SR. AF is a difficult condition in which to use 3D

and strain analysis. In our study, AF was present in 38 patients during the first TTE, and in 13 patients during the second TTE (Fig. 2). All patients had 3D and strain acquisition, but not all data were interpretable, because of artefacts or echogenicity. 3D analysis was possible in 68.8–72.9% of cases, and strain analysis in 83.3–100%. Currently development of 3D allows single beat acquisition, thus extending the use of 3D to patients with AF. Furthermore, the intraobserver and interobserver variability showed good results for strain and 3D analysis (Table A.2). It is also interesting to note that RA strain (concordance correlation coefficient ± standard error, 0.96 ± 0.03) and LA strain (0.95 ± 0.03) had the lowest interobserver variability among all atrial measures (Table A.2). This result may be explained by the semiautomated software analysis, which increases interobserver reproducibility.

Study limitations

First, the rate of AF recurrence is likely to have been underestimated, given the absence of Holter monitoring. However, with evaluation of rhythm during TTE at 6 months, we had a global assessment of the evolution of rhythm. Second, with a 6-month follow-up, our results need to be confirmed with longer clinical and echocardiography follow-up. Third, we evaluated biatrial remodelling only with TTE imaging; it would be interesting to have complementary data with MRI. However, most patients in our study were in AF during the first TTE, which can make interpretation of the MRI more difficult. Finally, concerning the software used for the strain analysis, we used LV-dedicated software. Our results will improve with the current development of strain and 3D software specific for RA/LA analysis. Furthermore, in our study, strain analysis software used seven-segment models and calculated global longitudinal strain with weighted combination of the regional strains. The atrial global strain could be refined with six-segment analysis rather than seven-segment analysis, and thus calculation according to the entire myocardial line length (following the speckle task force consensus [30, 31]).

Conclusions

By using 3D TTE and strain analysis, we evaluated reverse biatrial remodelling in patients with AF who were successfully cardioverted. We observed structural and functional remodelling, with a significant decrease in biatrial 3D volume and a significant improvement in biatrial global reservoir strain, 3D RAEF and 3D RAEI. It would be interesting to evaluate in a larger population sample

whether these new echocardiographic tools are useful for predicting rhythm outcome and long-term remodelling during follow-up in AF.

Acknowledgments

Editorial support was provided by Sophie Rushton-Smith (MedLink Healthcare Communications Limited), and was funded by the authors.

Sources of funding

This work was partially funded by Bayer.

Disclosure of interest

A.C. Research grants from **RESICARD** (research nurses) and the companies **ARS**, **Bayer** and **Boehringer-Ingelheim**. Consultant and lecture fees from the companies **AstraZeneca**, **Bayer Pharma**, **BMS-Pfizer Alliance**, **Boehringer-Ingelheim**, **Daiichi Sankyo** and **Novartis**, unrelated to the present work.

The other authors declare that they have no conflicts of interest concerning this article.

References

[1] Vaziri SM, Larson MG, Benjamin EJ, Levy D. Echocardiographic predictors of nonrheumatic atrial fibrillation. The Framingham Heart Study. Circulation 1994;89:724-30.

[2] Thomas L, Abhayaratna WP. Left Atrial Reverse Remodeling: Mechanisms, Evaluation, and Clinical Significance. JACC Cardiovasc Imaging 2017;10:65-77.

[3] Kirchhof P, Benussi S, Kotecha D, et al. 2016 ESC Guidelines for the management of atrial fibrillation developed in collaboration with EACTS. Eur Heart J 2016;37:2893-962.

[4] Nattel S, Harada M. Atrial remodeling and atrial fibrillation: recent advances and translational perspectives. J Am Coll Cardiol 2014;63:2335-45.

[5] Goette A, Kalman JM, Aguinaga L, et al. EHRA/HRS/APHRS/SOLAECE expert consensus on atrial cardiomyopathies: definition, characterization, and clinical implication. Europace 2016;18:1455-90.

[6] Jeevanantham V, Ntim W, Navaneethan SD, et al. Meta-analysis of the effect of radiofrequency catheter ablation on left atrial size, volumes and function in patients with atrial fibrillation. Am J Cardiol 2010;105:1317-26.

[7] Ma XX, Boldt LH, Zhang YL, et al. Clinical Relevance of Left Atrial Strain to Predict Recurrence of Atrial Fibrillation after Catheter Ablation: A Meta-Analysis. Echocardiography 2016;33:724-33.

[8] Leong DP, Joyce E, Debonnaire P, et al. Left Atrial Dysfunction in the Pathogenesis of Cryptogenic Stroke: Novel Insights from Speckle-Tracking Echocardiography. J Am Soc Echocardiogr 2017;30:71-9 e1.

[9] Pathan F, Sivaraj E, Negishi K, et al. Use of Atrial Strain to Predict Atrial Fibrillation After Cerebral Ischemia. JACC Cardiovasc Imaging 2017:Epub ahead of print.

[10] Muller H, Noble S, Keller PF, et al. Biatrial anatomical reverse remodelling after radiofrequency catheter ablation for atrial fibrillation: evidence from real-time three-dimensional echocardiography. Europace 2008;10:1073-8.

[11] Wylie JV, Jr., Peters DC, Essebag V, Manning WJ, Josephson ME, Hauser TH. Left atrial function and scar after catheter ablation of atrial fibrillation. Heart Rhythm 2008;5:656-62.

[12] Lang RM, Badano LP, Mor-Avi V, et al. Recommendations for cardiac chamber quantification by echocardiography in adults: an update from the American Society of Echocardiography and

the European Association of Cardiovascular Imaging. J Am Soc Echocardiogr 2015;28:1-39 e14.

[13] Pathan F, D'Elia N, Nolan MT, Marwick TH, Negishi K. Normal Ranges of Left Atrial Strain by Speckle-Tracking Echocardiography: A Systematic Review and Meta-Analysis. J Am Soc Echocardiogr 2017;30:59-70 e8.

[14] Hoit BD. Left atrial size and function: role in prognosis. J Am Coll Cardiol 2014;63:493-505.

[15] Cameli M, Mandoli GE, Loiacono F, Sparla S, Iardino E, Mondillo S. Left atrial strain: A useful index in atrial fibrillation. Int J Cardiol 2016;220:208-13.

[16] Beukema WP, Elvan A, Sie HT, Misier AR, Wellens HJ. Successful radiofrequency ablation in patients with previous atrial fibrillation results in a significant decrease in left atrial size. Circulation 2005;112:2089-95.

[17] Liu Z, Ling Z, Su L, et al. The effect of different treatment strategies on left atrial size in patients with lone paroxysmal atrial fibrillation-a prospective cohort study. J Interv Card Electrophysiol 2008;23:167-73.

[18] Reant P, Lafitte S, Jais P, et al. Reverse remodeling of the left cardiac chambers after catheter ablation after 1 year in a series of patients with isolated atrial fibrillation. Circulation 2005;112:2896-903.

[19] Choi JI, Park SM, Park JS, et al. Changes in left atrial structure and function after catheter ablation and electrical cardioversion for atrial fibrillation. Circ J 2008;72:2051-7.

[20] Rodrigues AC, Scannavacca MI, Caldas MA, et al. Left atrial function after ablation for paroxysmal atrial fibrillation. Am J Cardiol 2009;103:395-8.

[21] Tops LF, Bax JJ, Zeppenfeld K, Jongbloed MR, van der Wall EE, Schalij MJ. Effect of radiofrequency catheter ablation for atrial fibrillation on left atrial cavity size. Am J Cardiol 2006;97:1220-2.

[22] Verma A, Kilicaslan F, Adams JR, et al. Extensive ablation during pulmonary vein antrum isolation has no adverse impact on left atrial function: an echocardiography and cine computed tomography analysis. J Cardiovasc Electrophysiol 2006;17:741-6.

[23] Delgado V, Vidal B, Sitges M, et al. Fate of left atrial function as determined by real-time three-dimensional echocardiography study after radiofrequency catheter ablation for the treatment of atrial fibrillation. Am J Cardiol 2008;101:1285-90.

[24] Marsan NA, Tops LF, Holman ER, et al. Comparison of left atrial volumes and function by real-time three-dimensional echocardiography in patients having catheter ablation for atrial fibrillation with persistence of sinus rhythm versus recurrent atrial fibrillation three months later. Am J Cardiol 2008;102:847-53.

[25] Montserrat S, Sitges M, Calvo N, et al. Effect of repeated radiofrequency catheter ablation on left atrial function for the treatment of atrial fibrillation. Am J Cardiol 2011;108:1741-6.

[26] Schaaf M, Andre P, Altman M, et al. Left atrial remodelling assessed by 2D and 3D echocardiography identifies paroxysmal atrial fibrillation. Eur Heart J Cardiovasc Imaging 2017;18:46-53.

[27] Sanfilippo AJ, Abascal VM, Sheehan M, et al. Atrial enlargement as a consequence of atrial fibrillation. A prospective echocardiographic study. Circulation 1990;82:792-7.

[28] Prabhu S, Voskoboinik A, McLellan AJA, et al. A comparison of the electrophysiologic and electroanatomic characteristics between the right and left atrium in persistent atrial fibrillation: Is the right atrium a window into the left? J Cardiovasc Electrophysiol 2017;28:1109-16.

[29] Therkelsen SK, Groenning BA, Svendsen JH, Jensen GB. Atrial and ventricular volume and function evaluated by magnetic resonance imaging in patients with persistent atrial fibrillation before and after cardioversion. Am J Cardiol 2006;97:1213-9.

[30] Badano LP, Kolias TJ, Muraru D, et al. Standardization of left atrial, right ventricular, and right atrial deformation imaging using two-dimensional speckle tracking echocardiography: a consensus document of the EACVI/ASE/Industry Task Force to standardize deformation imaging. Eur Heart J Cardiovasc Imaging 2018;19:591-600.

[31] Voigt JU, Pedrizzetti G, Lysyansky P, et al. Definitions for a common standard for 2D speckle tracking echocardiography: consensus document of the EACVI/ASE/Industry Task Force to standardize deformation imaging. Eur Heart J Cardiovasc Imaging 2015;16:1-11.

Figure legends

Figure 1 Evaluation of LA strain (A) before and (B) after electrical cardioversion in the same patient, using QRS complex of zero as reference point. A. Only reservoir strain (RS) was recorded in atrial fibrillation. B. RS, conduit strain (CdS) and contractile strain (CtS) (reappearance in B of a second deflection [arrow] of the atrial strain curve) were recorded in patients in sinus rhythm. Note the improvement in longitudinal strain in the four-chamber view, before and after electrical cardioversion (red, +11.7% in A; red, +47.7% in B).

Figure 2 Cardiac rhythm evolution between inclusion and 6-month follow-up. AF: atrial fibrillation; FailCV: failed cardioversion; SponCV: spontaneous cardioversion; SR: sinus rhythm; SuccCV: successful cardioversion; TTE: transthoracic echocardiography.

Figure 3 Evolution of global longitudinal right atrial strain (left panel) and mean global longitudinal left atrial strain function (right panel) between baseline and 6-month follow-up, according to cardiac rhythm outcome. Error bars indicate standard error. FailCV: failed cardioversion; LA: left atrial; RA: right atrial; SponCV: spontaneous cardioversion; SuccCV: successful cardioversion.

Table 1 Evolution of three-dimensional atrial volumes during follow-up.

	At baseline (M0)	At 6 months (M6)	P^a
Right atrium			
SR-SR (n = 10)			
Max 3D RA Vol_i (mL/m^2) (n = 9)	31.4 ± 6.3	26.4 ± 3.1	0.24
Min 3D RA Vol_i (mL/m^2) (n = 9)	18.0 ± 4.6	15.9 ± 1.5	0.55
AF-SR (n = 25)			
Max 3D RA Vol_i (mL/m^2) (n = 16)	33.3 ± 2.70	26.9 ± 2.00	0.020
Min 3D RA Vol_i (mL/m^2) (n = 16)	21.5 ± 2.0	14.6 ± 1.2	0.0008
AF-AF (n = 13)			
Max 3D RA Vol_i (mL/m^2) (n = 8)	40.1 ± 4.6	45.3 ± 5.1	0.19
Min 3D RA Vol_i (mL/m^2) (n = 8)	28.9 ± 3.5	32.7 ± 4.0	0.18
Left atrium			
SR-SR (n = 10)			
Max 3D LA Vol_i (mL/m^2) (n = 9)	37.1 ± 2.9	34.6 ± 1.9	0.32
Min 3D LA Vol_i (mL/m^2) (n = 9)	17.5 ± 2.5	14.2 ± 1.4	0.32
AF-SR (n = 25)			
Max 3D LA Vol_i (mL/m^2) (n = 17)	45.2 ± 2.6	37.9 ± 2.5	0.001
Min 3D LA Vol_i (mL/m^2) (n = 17)	27.3 ± 2.3	20.3 ± 2.1	0.0021
AF-AF (n = 13)			
Max 3D LA Vol_i (mL/m^2) (n = 9)	48.3 ± 5.2	50.9 ± 5.4	0.063
Min 3D LA Vol_i (mL/m^2) (n = 9)	34.2 ± 3.8	34.1 ± 4.2	0.97

Data are expressed as mean ± standard error. 3D: three-dimensional; AF: atrial fibrillation; AF-AF: AF at M0 and AF at M6; AF-SR: AF at M0 and SR at M6; Max 3D LA Vol_i: body surface area-indexed maximal three-dimensional left atrium volume; Max 3D RA Vol_i: body surface area-indexed maximal three-dimensional right atrium volume; Min 3D LA Vol_i: body surface area-indexed minimal three-dimensional left atrium volume; Min 3D RA Vol_i: body surface area-indexed minimal three-dimensional right atrium volume; SR: sinus rhythm; SR-SR: SR at M0 and SR at M6.

[a] *P* values derived from the paired *t*-test.

Table 2 Evolution of three-dimensional atrial function during follow-up.

	At baseline (M0)	At 6 months (M6)	P^a
Right atrium			
SR-SR (n = 10)			
3D RAEF (%) (n = 9)	45.9 ± 15.3	38.0 ± 4.4	0.095
3D RAEI (%) (n = 9)	96.7 ± 18.6	68.6 ± 13.0	0.13
AF-SR (n = 25)			
3D RAEF (%) (n = 16)	34.3 ± 4.0	44.2 ± 4.3	0.037
3D RAEI (%) (n = 16)	65.2 ± 15.3	96.4 ± 15.4	0.034
AF-AF (n = 13)			
3D RAEF (%) (n = 8)	27.3 ± 4.4	27.7 ± 2.1	0.87
3D RAEI (%) (n = 8)	42.5 ± 4.5	54.3 ± 8.9	0.73
Left atrium			
SR-SR (n = 10)			
3D LAEF (%) (n = 9)	53.6 ± 4.5	58.2 ± 4.3	0.51
3D LAEI (%) (n = 9)	131.4 ± 21.1	172.8 ± 44.5	0.46
AF-SR (n = 25)			
3D LAEF (%) (n = 17)	40.6 ± 2.8	46.9 ± 3.8	0.18
3D LAEI (%) (n = 17)	75.4 ± 9.8	103.5 ± 13.5	0.078
AF-AF (n = 13)			
3D LAEF (%) (n = 9)	29.3 ± 2.3	33.6 ± 3.6	0.14
3D LAEI (%) (n = 9)	42.5 ± 4.5	54.3 ± 8.9	0.12

Data are expressed as mean ± standard error. 3D: three-dimensional; AF: atrial fibrillation; AF-AF: AF at M0 and AF at M6; AF-SR: AF at M0 and SR at M6; LAEF: left atrial emptying fraction; LAEI: left atrial expansion index; RAEF: right atrial emptying fraction; RAEI: right atrial expansion index; SR: sinus rhythm; SR-SR: SR at M0 and SR at M6.

[a] *P*-values derived from the paired *t*-test.

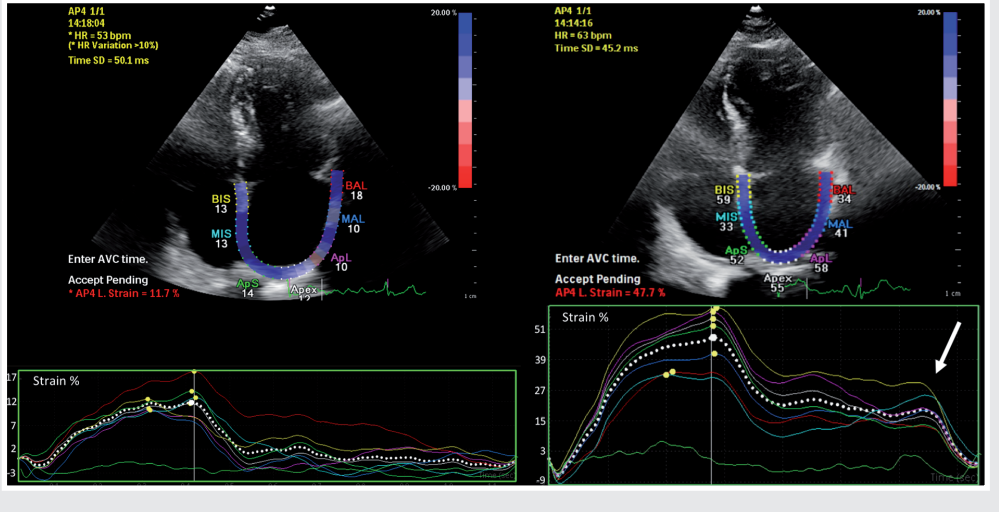
Atrial fibrillation
Sinus rhythm
AP4 1/1
14:18:04
* HR = 53 bpm
(* HR Variation >10%)
Time SD = 50.1 ms
20.00 %
-20.00 %
BIS 13
BAL 18
MAL 10
MIS 13
ApL 10
ApS 14
Apex
Enter AVC time.
Accept Pending
* AP4 L. Strain = 11.7 %
Strain %
17
12
7
2
-3
AP4 1/1
14:14:16
HR = 63 bpm
Time SD = 45.2 ms
20.00 %
-20.00 %
BIS 59
BAL 34
MIS 33
MAL 41
ApS 52
ApL 58
Apex 55
Enter AVC time.
Accept Pending
AP4 L. Strain = 47.7 %
Strain %
51
39
27
15
3
-9
QRS
T
P
Strain (%)
+
0
-
RS
CdS
CtS

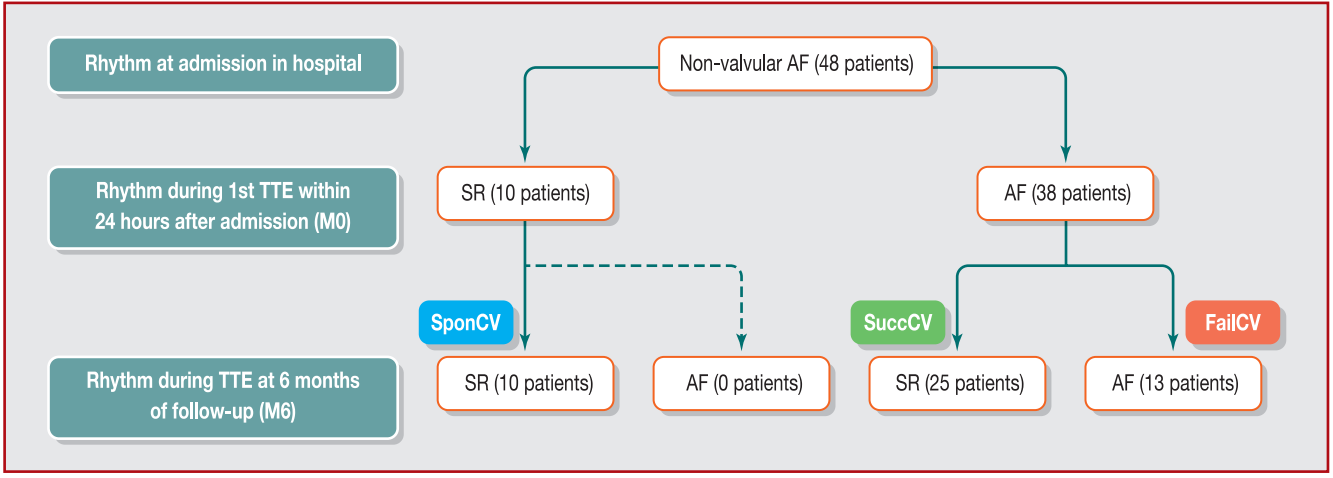
Rhythm at admission in hospital
Non-valvular AF (48 patients)
Rhythm during 1st TTE within 24 hours after admission (M0)
SR (10 patients)
AF (38 patients)
SponCV
SuccCV
FailCV
Rhythm during TTE at 6 months of follow-up (M6)
SR (10 patients)
AF (0 patients)
SR (25 patients)
AF (13 patients)

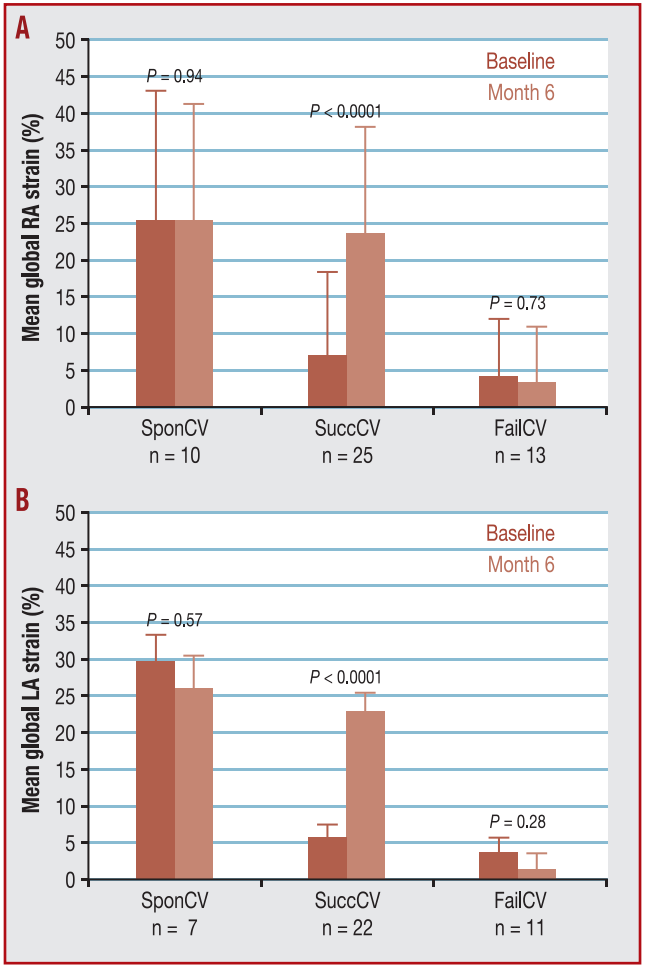
A
Mean global RA strain (%)
50
45
40
35
30
25
20
15
10
5
0
Baseline
Month 6
P = 0.94
P < 0.0001
P = 0.73
SponCV
n = 10
SuccCV
n = 25
FailCV
n = 13
B
Mean global LA strain (%)
50
45
40
35
30
25
20
15
10
5
0
Baseline
Month 6
P = 0.57
P < 0.0001
P = 0.28
SponCV
n = 7
SuccCV
n = 22
FailCV
n = 11

Table A.1 Baseline characteristics.

	SR-SR (n = 10)	AF-SR (n = 25)	AF-AF (n = 13)	P
Male sex	6 (60.0)	19 (76.0)	11 (84.6)	0.37
Age (years)	56.9 ± 11.8	65.0 ± 9.4	62.8 ± 14.8	0.18
BMI (kg/m^2)	25.1 (23.8–29.8)	27.8 (26.0–30.2)	26.2 (23.5–28.7)	0.24
Body surface area (m^2)	1.97 (1.76–2.03)	2.04 (1.93–2.16)	2.03 (1.91–2.12)	0.31
Systolic BP (mmHg)	119 (113–138)	136 (123–154)	129 (124–131)	0.20
Diastolic BP (mmHg)	81 (75–91)	81 (76–100)	88 (75–91)	0.82
Heart rate (beats/min)	113 (86–125)	93 (78–123)	78 (65–98)	0.08
Cardiovascular risk factors				
Hypertension	5 (50.0)	12 (45.0)	7 (53.8)	0.94
Diabetes	1 (10.0)	6 (24.0)	2 (15.4)	0.70
Hypercholesterolaemia	5 (50.0)	8 (32.0)	2 (15.4)	0.23
Hypertriglyceridaemia	2 (20.0)	4 (16.0)	2 (15.4)	0.95
Smoking status				0.99
Never	5 (50.0)	14 (56.0)	7 (53.8)	
Current	2 (20.0)	5 (20.0)	2 (15.4)	
Past	3 (30.0)	6 (24.0)	4 (30.8)	
Alcohol abuse	1 (10.0)	2 (8.0)	4 (30.8)	0.16
Medical history				
AF	0	8 (32.0)	7 (53.8)	0.017
Heart failure	0	0	4 (30.8)	0.005
Stroke	0	3 (12.0)	2 (15.4)	0.69
Coronary heart disease	2 (20.0)	4 (16.0)	1 (7.7)	0.76
Thromboembolism	0	1 (4.0)	1 (7.7)	0.66
Cancer	0	5 (20.0)	1 (7.7)	0.37
Patterns of AF at admission				<0.0001
Paroxysmal AF	8 (80.0)	2 (8.0)	0	

Persistent AF	2 (20.0)	23 (92.0)	13 (100)	
AF during first TTE	0	25 (100)	13 (100)	–
AF during second TTE	0	0	13 (100)	–
CHA_2DS_2-VASc score				0.67
0	1 (10.0)	5 (20.0)	1 (7.7)	
1	3 (30.0)	3 (12.0)	3 (23.1)	
≥ 2	6 (60.0)	17 (68.0)	9 (69.2)	
Biology at admission				
B-type natriuretic peptide (ng/L)	121 (47–186)	205 (80–311)	269 (145–464)	0.06
Troponin (µg/L)	0.04 (0.04–0.04)	0.04 (0.04–0.04)	0.04 (0.04–0.04)	0.81
C-reactive protein (mg/L)	3.0 (3.0–3.0)	3.0 (3.0–5.0)	3.0 (3.0–7.2)	0.40
D-dimer (ng/mL)	270 (247–413)	448 (270–881)	270 (243–375)	0.15
Echocardiography at M0 (common features)				
LVEF				0.89
LVEF ≥ 50%	7 (70.0)	17 (68.0)	9 (69.2)	
LVEF 40–49%	2 (20.0)	4 (16.0)	1 (7.7)	
LEVF < 40%	1 (10.0)	4 (16.0)	3 (23.1)	
Average e' (m/s)	0.09 (0.07–0.10)	0.09 (0.08–0.12)	0.10 (0.08–0.11)	0.56
E/e'	9.3 (5.5–11.0)	9.3 (7.5–10.7)	8.9 (7.1–10.1)	0.87
LA area > 20 cm^2	7 (70.0)	23 (92.0)	13 (100)	0.05
LA Vol_i (mL/m^2)	39.1 (28.3–46.5)	41.3 (33.9–47.3)	40.4 (37.1–52.3)	0.53
RA area (cm^2)	17.4 (13.5–22.2)	19.7 (18.1–24.3)	23.8 (18.8–27.4)	0.28
RA Vol_i (mL/m^2)	20.2 (13.9–37.7)	29.3 (21.5–39.7)	37.7 (16.5–47.1)	0.35
Ablation during follow-up	2 (20.0)	4 (16.0)	2 (15.4)	0.99
Treatment at discharge				
Antiarrhythmic drugs	6 (60.0)	20 (80.0)	7 (53.9)	0.21
Warfarin	4 (40.0)	9 (36.0)	8 (61.5)	0.34
Oral anticoagulant	6 (60.0)	14 (56.0)	5 (38.5)	0.59

Data are expressed as number (%), mean ± standard deviation or median (25^{th}–75^{th} percentiles). AF: atrial

fibrillation; AF-AF: AF at M0 and AF at M6; AF-SR: AF at M0 and SR at M6; BMI: body mass index; BNP: B-type natriuretic peptide; BP: blood pressure; CHA_2DS_2-VASc: congestive heart failure, hypertension, age ≥ 75 years (doubled), diabetes mellitus, stroke/transient ischaemic attack/thromboembolism (doubled), vascular disease, age 65–74 years, sex category (female); LVEF: left ventricular ejection fraction; e': mitral annular early diastolic velocity; E/e': mitral inflow velocity and mitral annular early diastolic velocity ratio; LA: left atrial; LA Vol_i: body surface area-indexed left atrial volume; M0: baseline; M6: 6-month follow-up; RA: right atrial; RA Vol_i: body surface area-indexed right atrial volume; SR: sinus rhythm; SR-SR: SR at M0 and SR at M6; TTE: transthoracic echocardiography.

Table A.2 Intraobserver and interobserver reproducibility of three-dimensional atrial volumes and atrial strain (n = 10).

	Intraobserver reproducibility		Interobserver reproducibility	
	Bias (95% LOA)	CCC ± SE	Bias (95% LOA)	CCC ± SE
Max 3D RA Vol_i	3.98 (–5.00; 12.96)	0.95 ± 0.02	6.47 (–8.91; 21.85)	0.72 ± 0.16
Min 3D RA Vol_i	2.87 (–5.40; 11.15)	0.90 ± 0.06	1.95 (–9.23; 13.13)	0.76 ±0.14
Global RA strain	1.30 (–3.56; 6.16)	0.95 ± 0.03	–1.10 (–11.49; 9.30)	0.96 ± 0.03
Max 3D LA Vol_i	0.72 (–5.95; 7.43)	0.88 ± 0.07	–0.73 (–17.76; 16.31)	0.68 ± 0.15
Min 3D LA Vol_i	1.41 (–6.05; 8.87)	0.92 ± 0.05	–2.06 (–15.55; 11.42)	0.89 ± 0.06
Mean global LA strain	1.44 (–8.37–11.25)	0.98 ± 0.01	–2.22 (–9.17; 4.74)	0.95 ± 0.03

3D: three-dimensional; CCC: concordance correlation coefficient; LA: left atrial; LOA: limits of agreement; Max 3D LA Vol_i: body surface area-indexed maximal three-dimensional left atrial volume; Max 3D RA Vol_i: body surface area-indexed maximal three-dimensional right atrial volume; Min 3D LA Vol_i: body surface area-indexed minimal three-dimensional left atrial volume; Min 3D RA Vol_i: body surface area-indexed minimal three-dimensional right atrial volume; RA: right atrial; SE: standard error.